Pathology - Research and Practice 227 (2021) 153643

Contents lists available at ScienceDirect

Pathology - Research and Practice

journal homepage: www.elsevier.com/locate/prp

HER2 promotes epithelial-mesenchymal transition through regulating osteopontin in gastric cancer

Yalan Liu [a,b], Lingli Chen [a,b], Dongxian Jiang [a,b], Lijuan Luan [a,b], Jie Huang [a,b], Yingyong Hou [a,b,*], Chen Xu [a,b,*]

[a] Department of Pathology, Zhongshan Hospital, Fudan University, Shanghai, China
[b] Department of Pathology, School of Basic Medical Sciences & Zhongshan Hospital, Fudan University, Shanghai, China

ARTICLE INFO

Keywords:
HER2
Osteopontin
Epithelial-mesenchymal transition
Gastric cancer

ABSTRACT

Aims: HER2 and osteopontin (OPN) are both important biomarkers in gastric cancer (GC). The relationships between them remain to be revealed. The purpose of this study is to explore the role of OPN in epithelial-mesenchymal transition (EMT) in HER2 positive GCs.

Methods: Nanostring analysis was used to compare the mRNA levels of 730 cancer related genes between paired HER2 3+ and non-3+ areas in GC patients. Immunohistochemistry (IHC) staining was performed to analyze the expression levels of OPN, as well as EMT markers including E-cad, N-cad, twist and vimentin in both areas. To further verify the role of OPN in EMT, the expression levels of OPN and EMT markers, tumor invasion/migration were analyzed after down-regulating HER2 and OPN in GC cell lines MKN-45 and N-87.

Results: Nanostring analysis identified 8 differential expression genes between HER2 3+ and non-3+ areas. Among them, the expression level of OPN was positively correlated with that of HER2. In GC specimens, OPN showed higher expression level in HER2 3+ areas where higher E-cad expression levels and lower N-cad and twist levels were also found. After knocking down OPN and HER2 by siRNA, both cell lines show decreased invasion/migration abilities, along with the down-regulation of the EMT phenotype, supporting by the decrease of E-cad, and the increase of N-cad and twist at both mRNA and protein levels. In addition, HER2 knock-down lead to a dramatic decrease of OPN expression.

Conclusions: These findings indicate that HER2 may promote EMT *via* the regulation of OPN in GCs.

1. Introduction

Gastric cancer (GC) is the fifth most common cancer and the third most common cause of cancer-related death in the world [1,2]. In China, it remains the second and third most common malignancy in male and female respectively, and the second leading cause of cancer death in both genders [3]. Human epidermal growth receptor 2 (HER2) is an important biomarker in GCs as a vital predictive biomarker to select eligible candidates for the anti-HER2 molecular targeted therapy [4].

HER2 is overexpressed in 10–20% of GCs. Heterogeneity is an important characteristic of HER2 expression in GCs. Studies show that the heterogeneity can be found in 30.0–79.3% of HER2 positive GCs [5–7]. Currently, little is known about cause of HER2 heterogeneity, as well as its roles in tumor genesis and development in GCs [8]. To better understand the heterogeneity, in this study, 730 tumor-related genes were compared between paired HER2 positive areas and negative areas in HER2 positive GCs. Several genes were identified to show differential expression between the two areas, and among them, SPP1 expression exhibited a positive correlation with HER2.

Osteopontin (OPN), encoding by SPP1, is a secretory extracellular matrix (ECM) protein involving in various physiological and pathophysiological processes including cell attachment, migration, invasion, proliferation, tissue remodeling, bone formation and inflammation [9–12]. OPN is expressed in many malignancies including GCs, participates and promotes tumor genesis, development, metastasis and immune response [13–15]. Inhibition of OPN expression levels could inhibit the growth and metastasis of GC cell lines [16]. Since OPN play such pivotal roles in various kinds of tumors, it is also regarded as a potential target for molecular targeted therapy and immune therapy [15,17].

Despite of all these findings, the relationships between HER2 and OPN remain largely unrevealed. Both of them indicate progressive

* Corresponding authors at: Department of Pathology, Zhongshan Hospital, Fudan University, Shanghai 20032, China.
E-mail addresses: houyingyong@aliyun.com (Y. Hou), xu.chen@zs-hospital.sh.cn (C. Xu).

https://doi.org/10.1016/j.prp.2021.153643
Received 30 May 2021; Received in revised form 24 September 2021; Accepted 30 September 2021
Available online 5 October 2021

behaviors. Furthermore, HER2 amplification promotes epithelial-mesenchymal transition (EMT) through the inhibition of GSK3β in GCs [18]. The correlation between OPN and HER2 indicated the possibility that OPN may involve in the HER2 mediated EMT process.

Therefore, in this study, the expression levels of OPN and EMT related markers were compared between the HER2 3+ areas and non-3+ areas. SPP1 and HER2 were knocked down respectively in GC cell lines to explore their roles in the EMT process. We hope the function of OPN in EMT in HER2 positive cancers could be revealed.

2. Materials and methods

2.1. Patients

From January 2015 to June 2015, a total of 549 cases of GC resected specimens were obtained in the Department of Pathology, Zhongshan Hospital, Fudan University. Evaluation of HER2 immunohistochemistry (IHC) status identified 68 HER2 3+ cases. Among them, 35 cases showed heterogeneous HER2 staining. These cases were subjected to the following tissue microarray analysis. Within the 35 cases, 6 cases with both HER2 3+ area and 0 area were further selected for the Nanostring analysis.

Patient characteristics including age, gender, Lauren classification, differentiation, pTNM stage (according to eighth edition of the Union for International Cancer Control (UICC) guidelines), *etc.* were collected. The research protocol was approved by the ethics board of Zhongshan Hospital, Fudan University.

2.2. Tissue microarray construction

Tissue microarrays (TMA) were constructed following previously described procedures [19]. Briefly, all the IHC sections of HER2 were reviewed and the HER2 3+ and non-3+ areas of each case were selected and marked. The corresponding regions were then marked on the formalin-fixed, paraffin-embedded (FFPE) blocks. The 3+ and non-3+ areas (3 mm in diameter and 6 mm long) were extracted from the blocks and planted vertically into the recipient block. The planting surface was aggregated on the aggregated machine.

2.3. Immunohistochemistry (IHC) analysis

IHC staining was performed on a BenchMark XT automated stainer (Ventana Medical Systems, Inc., Tucson, AZ) with the iView DAB Detection Kit (Ventana, Tucson, AZ) following the manufacturer`s instructions. The first antibodies were as follows: HER2 (4B5) rabbit monoclonal antibody (Ventana Medical Systems, Inc., Tucson, AZ), OPN (Santa Cruz, 1:500), E-cad (Abcam, 1:300), N-cad (Abcam, 1:200), twist (Abcam, 1:200), and Vimentin (Abcam, 1:500).

HER2 was scored based on the established criteria for resected specimens of GC [20–22]. Briefly, sections with no staining or positive staining on $<$ 10% tumor cells were considered a score of 0; those with faintly perceptible staining in only part of the tumor cell membrane in $\geq$ 10% tumor cells were scored 1+; samples with weak to moderate complete, basolateral or lateral membranous staining in $\geq$ 10% tumor cells were scored 2+; and those with strong complete, basolateral or lateral membranous staining were scored 3+.

Immunohistochemical scores (IHS) were applied to the evaluation of OPN, E-cad, N-cad, twist, and Vimentin [23]. The IHS was calculated by combining an estimate of the percentage of immunoreactive cells (quantity score) with an estimate of the staining intensity (intensity score). The quantity score was assessed as follows: no staining was scored as 0, 1–10% as 1, 11–50% as 2, 51–80% as 3, 81%–100% as 4. Staining intensity was rated on a scale of 0–3, with 0 = negative, 1 = weak, 2 = moderate, 3 = strong. The raw data were converted to the HIS by multiplying the quantity and intensity scores.

2.4. Nanostring analysis

Six HER2 positive GC cases with paired HER2 IHC 3+ and 0 areas were obtained. Both areas were marked on the paraffin blocks and obtained for the RNA extraction afterward. Total RNA was prepared with a FFPE DNA, RNA and DNA/RNA Kit (AmoyDx, China) after deparaffinization following the manufacturer`s manual. A Cancerpath panel including 730 genes was used in the analysis (Supplementary 1). The Nanostring analysis was performed in the Laboratory Testing Division (LTD) of Wuxi AppTec (Shanghai, China) following the protocols of nCounter XT CodeSet Gene Expression Assays (Wuxi AppTec, China). Briefly, firstly, a total of 100 ng RNA was subjected to hybridization at 65 °C for 18 h. Then the samples were processed on the nCounter Prep Station (Nanostring Tec.) following standard protocols. Once the processing was completed, the cartridge was removed for imaging on the nCounter Digital Analyzer (Nanostring Tec.). A detailed protocol of the Nanostring analysis was shown in the Supplementary 2. The data were analyzed with nSolve Analysis Software 3.0 (Nanostring Tec.) and were adjusted based on the internal control within the panel. Genes with the values twice as large or higher than negative controls were considered showing expression at the mRNA level. Genes were considered significant different when the expression levels varied by twofold or greater.

2.5. Cell culture

The GC cell lines NCI-N87 (ATCC CRL-5822TM) and MKN45 (JCRB0254) were obtained from American Type Culture Collection (Manassas, VA) and JCRB cell bank (Osaka, Japan), respectively, and were cultured in a 5% CO_2 incubator as recommended.

2.6. RNA interference

For small interfering RNA (siRNA)-mediated knockdown of SPP1 and HER2, cells were transfected with 100 nM of either the targeting or control siRNA using Lipofectamine 2000 (Invitrogen) for 24 or 36 h. The functional assays were subsequently done after validation of SPP1 and HER2 knockdown. Several independent duplexes of FAM labeled siRNAs (synthesized by Genepharma) were used to target each gene. The sequences of siRNA targeting human SPP1 were as follows: (1) Sense (5′-3′): CCUGUGCCAUACCAGUUAATT, Antisense (5′-3′): UUAACUGGUAUGGCACAGGTT; (2) Sense (5′-3′): GUCUCACCAUUCUGAUGAATT, Antisense (5′-3′): UUCAUCAGAAUGGUGAGACTT, (3) Sense (5′-3′): GGGAAGGACAGUUAUGAAATT, Antisense (5′-3′): UUUCAUAACUGUCCUUCCCTT. The sequences of siRNA that targeted HER2 were as follows: (1) Sense (5′-3′): GGGACGAAUUCUGCACAAUTT, Antisense (5′-3′): AUUGUGCAGAAUUCGUCCCTT; (2) Sense (5′-3′): GCAGUUACCAGUGCCAAUATT, Antisense (5′-3′): UAUUGGCACUGGUAACUGCTT; (3) Sense (5′-3′): CUGGCUCCGAUGUAUUUGATT, Antisense (5′-3′): UCAAAUACAUCGGAGCCAGTT. The sequences for negative control SiRNA were: Sense (5′-3′): UUCUCCGAACGUGUCACGUTT, Antisense (5′-3′): ACGUGACACGUUCGGAGAATT.

2.7. RNA extraction, complementary DNA preparation and real-time quantitative PT-PCR

Total RNA was extracted with TRIzol reagent (Invitrogen, USA) following the manufacturer`s instructions. The purity and integrity of RNA were assessed spectroscopically before use. Single-strand complementary DNA was prepared with 1 μg total RNA using the ReverTra Ace qPCR RT Kit (Toyobo, Japan) according to protocols as recommended.

The messenger RNA (mRNA) levels of HER2, SPN1, CDH1, CDH2, and twist were detected by real-time PCR (MX300P QPCR Systems, Agilent, USA). Glyceraldehyde-3-phosphate dehydrogenase (GAPDH) was used as an internal standard. The primers used were designed with Primer 3.0. PCR reactions were performed in a volume of 10 μl with SYBR Green Realtime PCR Master Mix (Toyobo, Japan). The data was

analyzed as previously described [24].

The sequences of the primers are as follows: SPP1: forward (5′-3′): ACTGATTTTCCCACGGACCT, reverse (5′-3′): CTCGCTTTCCATGTGTGAGG; HER2: forward (5′-3′): GGTGGTCTTTGGGATCCTCA, reverse (5′-3′): ACCTTCACCTTCCTCAGCTC; CDH1: forward (5′-3′): GTGGGCCAGGAAATCACATC, reverse (5′-3′): AGTGTCCCTGTTCCAGTAGC; CDH2: forward (5′-3′): CGGTTTCATTTGAGGGCACA, reverse (5′-3′): TTGGAGCCTGAGACACGATT; twist: forward (5′-3′): TCTTACGAGGAGCTGCAGAC, reverse (5′-3′): AGGAAGTCGATGTACCTGGC; GAPDH: forward (5′-3′): ATCATCCCTGCCTCTACTGG, reverse (5′-3′): CCTGCTTCACCACCTTCTTG.

2.8. Western blot

Cells were lysed and denatured at 95 °C for 5 min in sample buffer. Total protein was separated using sodium dodecyl sulfate (SDS)-polyacrylamide gel electrophoresis and transferred to polyvinylidene fluoride membranes. Membranes were blocked in phosphate buffered saline with 5% non-fat milk and 0.05% Tween-20 (Sigma-Aldrich, USA) for 1 h and then incubated in the primary antibodies at 4 °C overnight. After washing in phosphate-buffered saline, the membranes were incubated with peroxidase-conjugated secondary antibodies at room temperature for 1 h. The bands of targeted protein were detected by enhanced chemiluminescence (Pierce, USA).

The first antibodies for HER2 (Dako, A0485), Osteopontin (Abcam, ab69498), E-cadherin (Santa-cruz , sc7870), N-cadherin (Abcam, ab76011), twist (Abcam, ab49254) and Tublin (CWBIO, CW0098A) were diluted to 1:3000, 1:400, 1:250, 1:5000, 1:400 and 1:2000, respectively.

2.9. Cell invasion/migration assays

The invasion assays were performed with 24 well transwell chambers (Corning, NY). The 8 μm pore inserts were coated with 20 μl Matrigel (Becton Dickinson). The tumor cells were prepared in the serum free medium, and 5×10^4 cells/filter in 200 μl medium were added to the coated filters in triplicate. Next 500 μl of 10% fetal bovine serum (FBS) media was added to the lower compartments. The upper surface of the filters was wiped off with cotton swabs after 36 h incubation at 37 °C. Tumor cells that migrated through the filters were fixed and stained with 0.5% crystal violet, photographed, and counted. Five random images of the cells were selected, and cells in each image were counted and mean standard deviation values were calculated. The migration assays were conducted similarly, except that the inserts were not coated with Matrigel and the incubation time was 24 h.

2.10. Statistical analysis

Mean values were calculated and presented as mean ± SD. The means were compared with Student *t*-test and Mann-Whitney U between different groups. Spearman`s rank correlation was performed to assess the linear relationships between two parameters. The statistical package SPSS version 22.0 (SPSS, Chicago, IL, USA) was used for all the analyses. A P value of < 0.05 was defined as statistically significant.

3. Results

3.1. Patient characteristics

A total of 68 HER2 IHC 3+ cases were obtained from 549 GC cases. Among them, 35 cases were identified to show heterogeneous HER2 expression. There were 28 males and 7 females. The age span was 39–74 years old with a median of 60 and an average of 60.9. With regard to the Lauren classification, there were 26 intestinal type tumors, 4 diffuse type tumors and 5 mixed type tumors. Twenty-one cases located in the proximal part of stomach, and the other 14 cases located in the distal part. The maximum diameter of the tumors ranged from 1.2 to 16.0 cm with an average of 4.7 cm. The main clinicopathological characteristics were shown in Table 1.

Thirty-five pairs of tissue from the paired HER2 3+ and non-3+ areas were obtained, and subjected to tissue microarray construction that were used in subsequent IHC analysis. The HER2 status of the non-3+ areas were as follows: 0 in 24 cases, 1+ in 2 cases, and 2+ in 9 cases.

3.2. Nanostring analysis identified differential expression genes between HER2 3+ areas and HER2 0 areas

The mRNA levels of a total of 730 genes were analyzed and compared between the HER2 3+ areas and HER2 0 areas in 6 cases (Fig. 1A). Eight genes with significant differential expression (the levels varied by two folds or greater) between the two areas were identified and these genes were shared by ≥ 3/6 cases. Within them, 3 genes showed elevated expression levels in the HER2 3+ areas, including HER2, SPP1, and MMP9 (Fig. 2B). The other 5 genes showed decreased expression levels in the 3+ areas, including CARD1, DLL1, LAT, PDGFRA, and PLA2G10 (Fig. 2B). The correlation of the mRNA levels between HER2 and SPP1 was further analyzed, and a positive linear correlation was identified between the two genes ($r = 0.707$, $P = 0.01$) (Fig. 1C).

3.3. The expression of OPN and EMT related proteins in the HER2 3+ and non-3+ areas

The expression levels of OPN and 4 EMT related proteins (E-cad, N-cad, twist and vimentin) were analyzed and compared between the HER2 3+ and non-3+ areas by IHC in the 35 cases (Fig. 2). At the protein level, OPN demonstrated elevated expression in the 3+ areas comparing to the non-3+ areas, and this was consistent with findings at the mRNA levels from the Nanostring analysis. With regard to the EMT related proteins, both N-cad and twist exhibited higher expression in the 3+ areas, while E-cad showed lower expression in the same areas. No vimentin expression was identified in both HER2 3+ and non-3+ areas

Table 1
Patient characteristics.

	Patient number (%)
Total	35 (100)
Gender	
Male	28 (80.0)
Female	7 (20.0)
Differentiation	
Moderate	17 (48.6)
Poorly	18 (51.4)
Lauren	
Intestinal	26 (74.3)
Diffuse	4 (11.4)
Mixed	5 (14.3)
Location	
Proximal	21 (60.0)
Distal	14 (40.0)
Lymphatic metastasis	
Yes	25 (71.4)
No	10 (28.6)
Vessel invasion	
Yes	22 (62.9)
No	13 (37.1)
Nerve invasion	
Yes	19 (54.3)
No	16 (45.7)
Stage	
IA	4 (11.4)
IB	1 (2.9)
IIA	5 (14.3)
IIB	8 (22.9)
IIIA	5 (14.3)
IIIB	7 (20)
IIIC	5 (14.3)

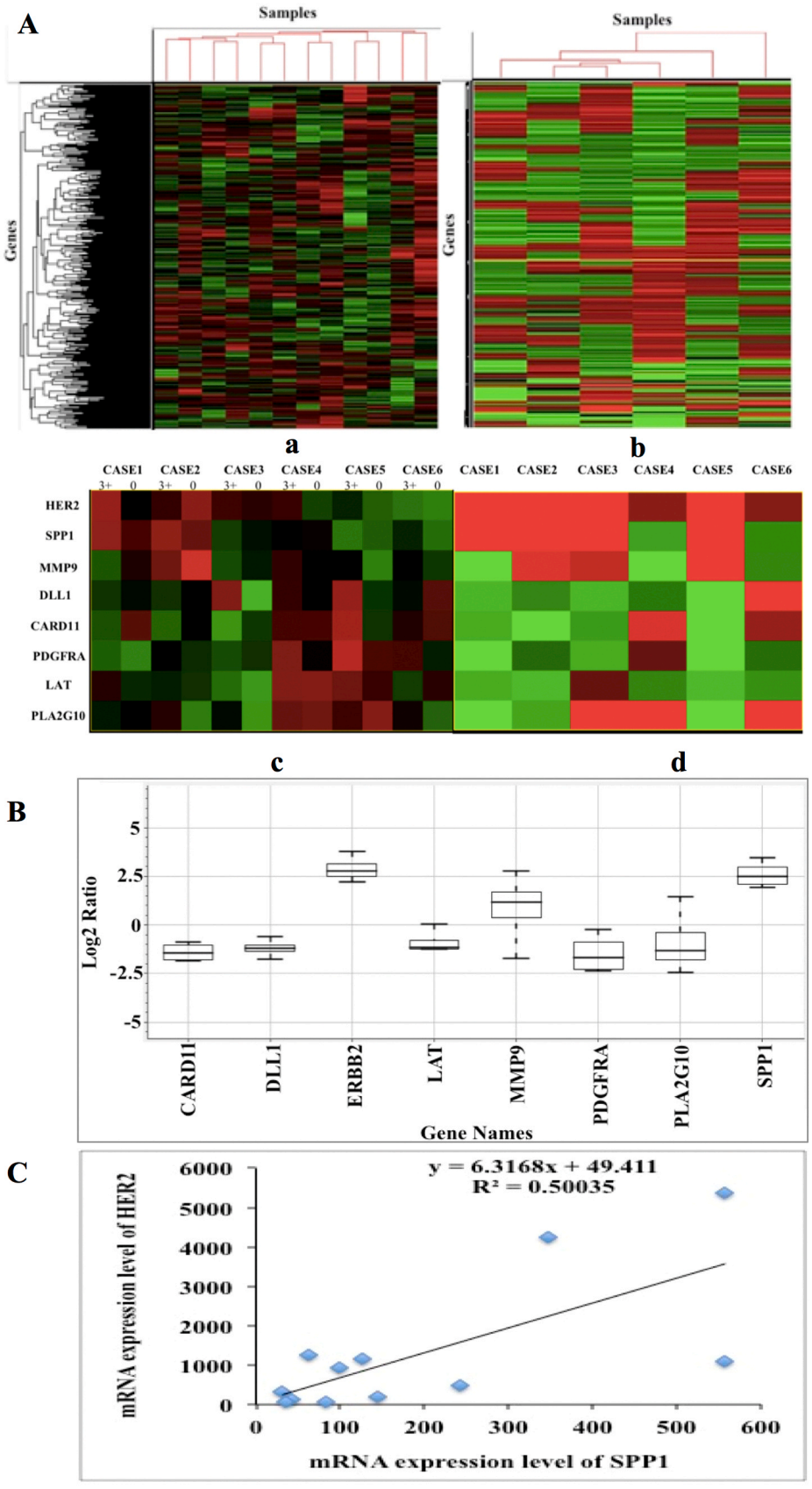

Fig. 1. Nanostring analysis. A Heat maps. a. Heat map of mRNA expression level of each gene. b. Heat map of the ratio of mRNA expression level between HER2 3+ area and 0 area. c. Heat map of mRNA expression levels of the differential expression genes. d. Heat map of the ratio of mRNA expression between HER2 3+ area and 0 area of the differential expression genes. B. Relative expression levels of the differential expression genes (3+ area/ 0 area). C. Linear correlation between HER2 and SPP1 mRNA expression ($P = 0.01$).

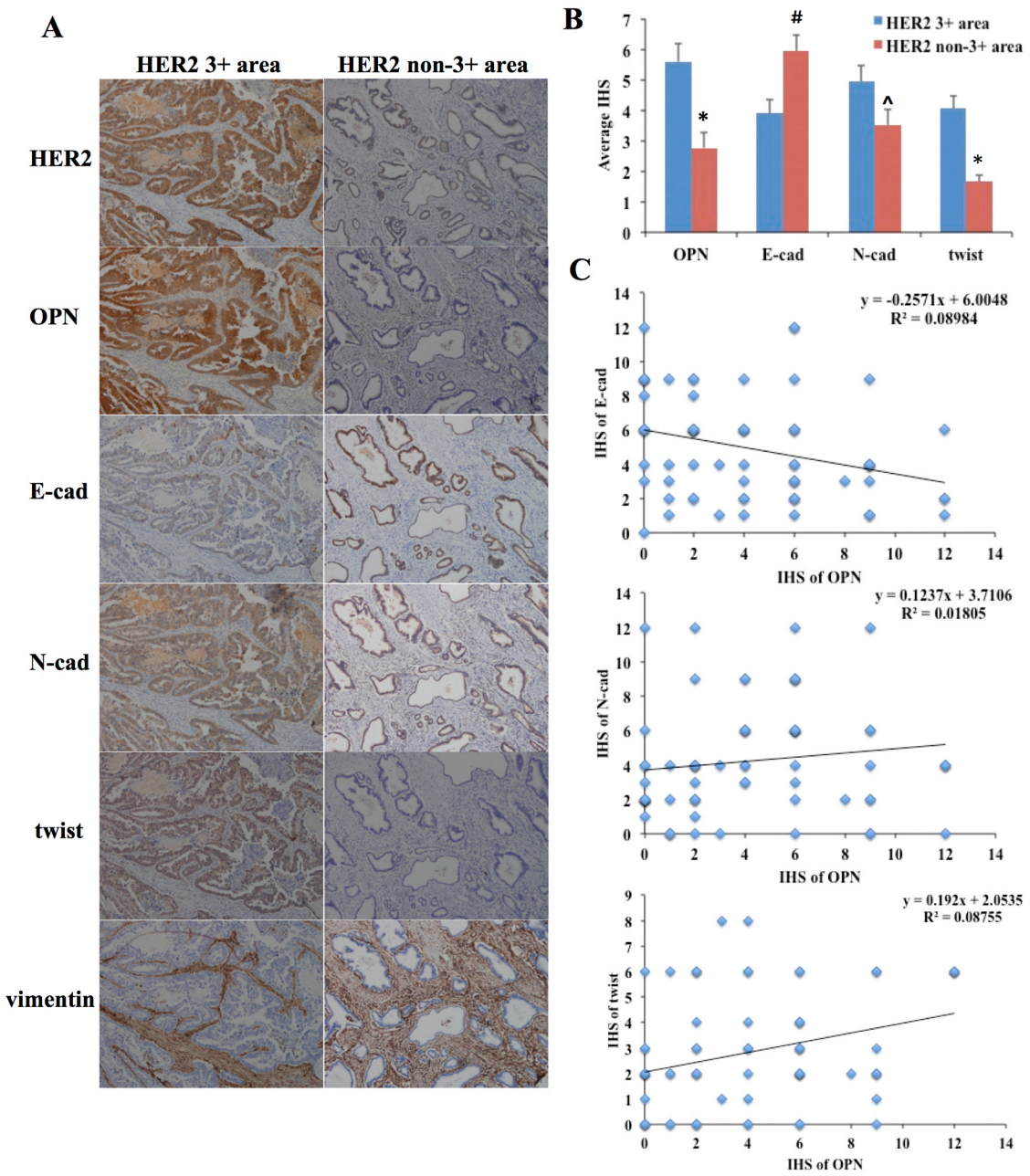

Fig. 2. IHC analysis of OPN and EMT related genes in the HER2 IHC 3+ and non-3+ area. A. IHC images of these genes in the 3+ and non-3+ areas in a representative case. The 3+ areas (left panel) showed higher OPN, N-cad twist levels and lower E-cad level than the non-3+ areas (right panel). Vimentin was negative in both areas. B. Comparison of immunohistochemical scores (IHS) of OPN, E-cad, N-cad, and twist between the two areas. *$P < 0.001$, #$P = 0.004$, ^$P = 0.049$. C. Correlations between OPN and E-cad, N-cad, or twist. There were a negative correlation between OPN and E-cad (n = 70, $r = 0.317$, $P = 0.008$), a positive correlation between OPN and N-cad (n = 70, $r = 0.234$, $P = 0.051$) and a positive correlation between OPN and twist (n = 70, $r = 0.283$, $P = 0.018$).

in all cases.

3.4. SiRNA interference down-regulated SPP1 and HER2 at mRNA levels

Human GC cell lines MKN45 and N87 were transiently transfected with FAM labeled siRNAs targeting SPP1 and HER2. Under fluorescence microscope, the fluorescence could be found in over 70% of the tumor cells, indicating that the siRNA had been successfully transfected (Fig. 3A, B). Real-time PCR analysis showed that the mRNA levels of SPP1 and HER2 were significantly down-regulated by all the 3 siRNAs. Two siRNA (siRNA1 and siRNA2) were chosen in the subsequent studies for their better performance in knocking down the targeted genes (Fig. 3C, D).

3.5. The effects of SPP1 knockdown on the expression of HER2 and EMT related genes

After knocking down SPP1 with siRNA transfection, SPP1, HER2 and the EMT related genes (CDH1, CDH2, and twist) were analyzed at the mRNA and protein levels (Fig. 4A, B).

In both MKN45 and N87 cell lines, SPP1 expression was significantly down-regulated at the mRNA level ($P < 0.001$) (Fig. 4A). HER2 expression did not show significant changes ($P > 0.05$) (Fig. 4A). With regard to the EMT related genes, the expression levels of CDH1 increased, while the levels of CDH2 and twist decreased significantly ($P < 0.001$) (Fig. 4A).

Those genes exhibited similar changes at the protein levels in both

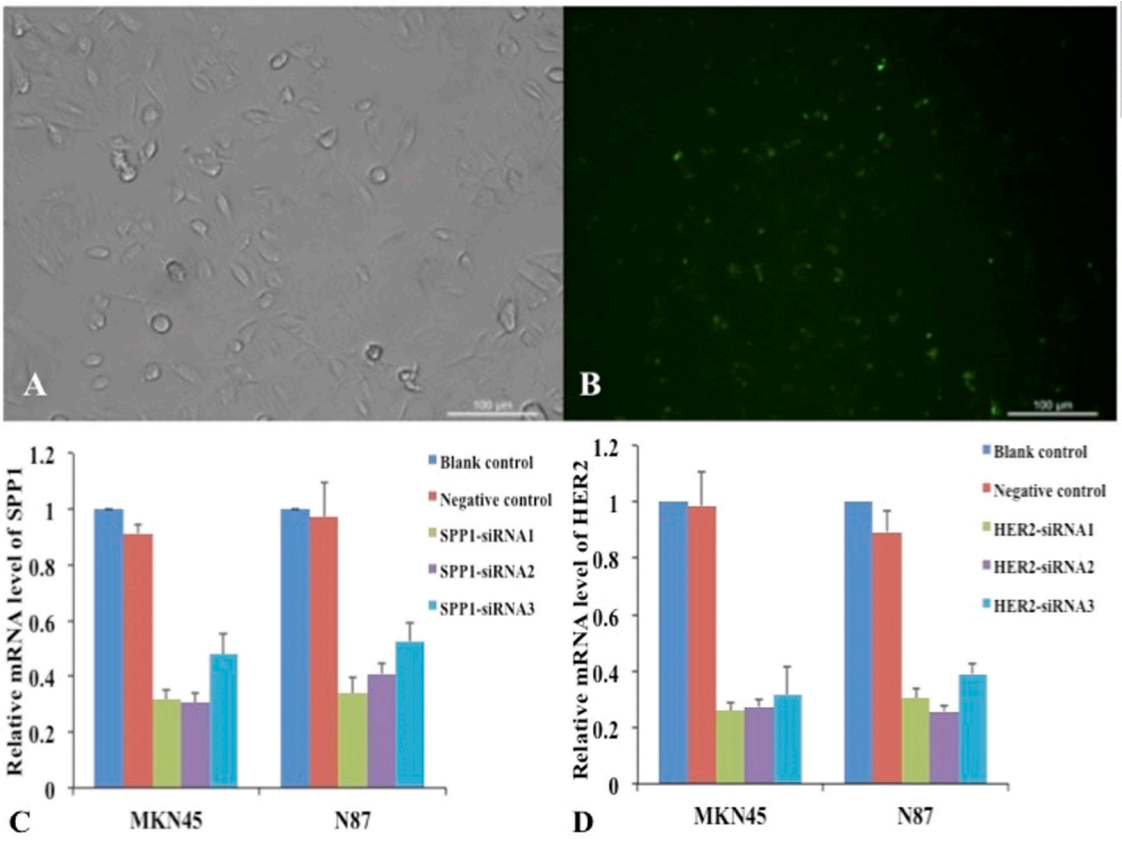

Fig. 3. Transient transfection and evaluation of transfection effect. A. N87 cells under light microscope after transfection (×100). B. Fluorescence image (×100). C. SPP1-siRNA. D. HER2-siRNA. All $P < 0.05$.

cell lines (Fig. 4B). After SPP1 knockdown, HER2 expression was not affected. As to the EMT related genes, E-cad expression increased at the protein level, meanwhile N-cad and twist expression decreased.

3.6. The effects of HER2 knockdown on the expression of SPP1 and EMT related genes

We next analyzed the expression of SPP1 and the above-mentioned EMT related genes after knocking down HER2 by siRNA transfection (Fig. 4C, D).

At the mRNA level, HER2 knockdown led to the decrease of HER2 and SPP1 expression in both cell lines ($P < 0.05$). With regard to the EMT genes, CDH1 expression level was up-regulated after HER2 knockdown, while CDH2 and twist expression was down-regulated significantly ($P < 0.05$).

The changes of these genes at protein level were consistent to those at the mRNA level after siRNA transfection in both cell lines.

3.7. Knockdown of SPP1 and HER2 inhibited the migration and invasion of GC cell lines

As shown in Fig. 5, SPP1 and HER2 knockdown significantly suppressed the migratory and invasive abilities in both MKN45 and N87 cell lines ($P < 0.05$).

4. Discussion

Among the 7 differential expression genes (except HER2) between HER2 3+ and non-3+ areas, 2 of them showed higher expression levels in the 3+ areas, including SPP1 and MMP-9. The relationships between MMP-9 and HER2 have been discussed previously. One study showed that HER2 knockdown resulted in the down-regulation of the expression of MMP-9 and whereas HER2 overexpression of improved the transcription of MMP-9 through the activation of its promoter [25].

The relationships between SPP1 and HER2 are still to be elucidated. OPN, encoded by SPP1, often shows high expression levels in GCs. The expression level of OPN was associated with various clinicopathological parameters. Overexpression of OPN was considered to be related to lower apoptosis, high proliferation, low grade, advanced stage, lymphatic metastasis, vessel invasion and distant metastasis [17,26–29]. Similarly, overexpression of HER2 in GCs is also more frequently seen in intestinal type, low grade, and advanced stage tumors [30]. Therefore, the expression of OPN and HER2 share some clinicopathologic characteristics in GCs. The overlapping of the expression profiles between HER2 and OPN, along with the positive correlation between the two genes at mRNA level, indicated the necessity to further explore the relationships between HER2 and OPN and their roles in HER2 positive GCs.

Our IHC analysis showed that OPN expression was higher in the HER2 3+ areas than in the non-3+ areas. This finding is consistent to the results of Nanostring analysis. The evaluation of expression profiles of EMT related genes indicated that neoplastic cells in the HER2 3+ areas showed the acquisition of EMT phenotype. These findings supported that HER2 amplification induced EMT in GCs. Previous studies indicated that HER2 participates in the process of EMT, and HER2 amplification can induce EMT through GSK3β pathway [18,31]. The consistency of OPN and HER2 expression, as well as the correlation between OPN and EMT markers indicated that OPN might be an important participant in the HER2 induced EMT process in GCs.

To confirm our hypothesis, we next knocked down SPP1 and HER2 respectively in MKN45 and N87 cell lines. After SPP1 knockdown, the EMT in both cell line was inhibited, showing loss of the EMT phenotype

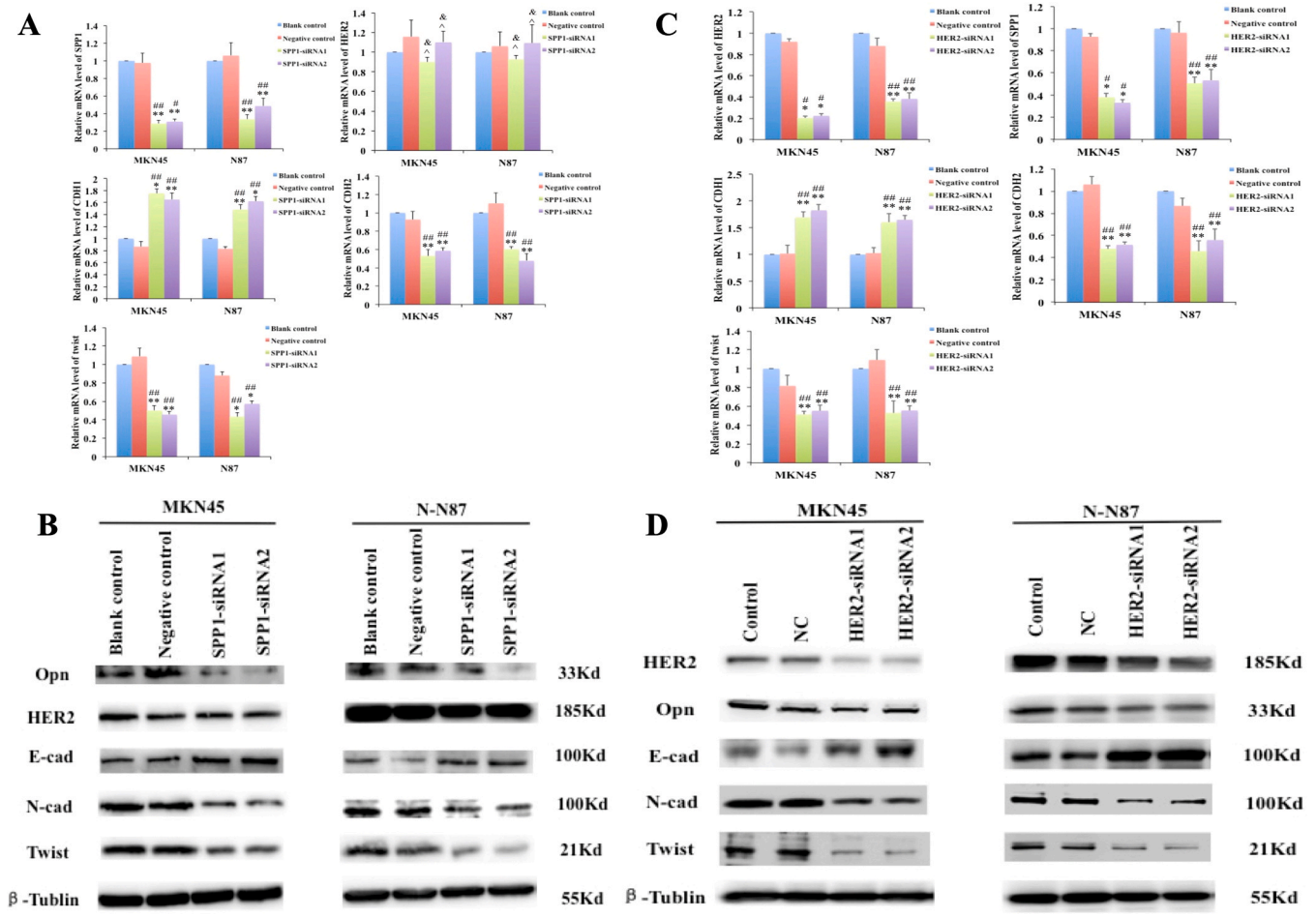

Fig. 4. The expression of OPN and EMT markers after the knockdown of OPN and HER2. A. After SPP1-siRNA transfection, the mRNA levels of SPP1, CDH2 and twist decreased, while CDH1 level increased in both cell lines. HER2 mRNA level did not show obvious changes after the transfection. $\#P < 0.001$*vs* Blank control, $\#\#P < 0.05$ *vs* Blank control, $\&P > 0.05$ *vs* Blank control, $*P < 0.001$*vs* Negative control, $**P < 0.05$ *vs* Negative control, $\hat{}P > 0.05$ *vs* Negative control B. Western blot analyses of OPN, HER2, and EMT markers in GC cell line MKN45 and N87 after SPP1-siRNA transfection. The changes of these genes at protein level were consistent with the mRNA level. C. After HER2-siRNA transfection, the mRNA level of HER2, SPP1, CDH2 decreased, meanwhile CDH1 level increased significantly in both cell lines. $\#P < 0.001$*vs* Blank control, $\#\#P < 0.05$ *vs* Blank control, $*P < 0.001$*vs* Negative control, $**P < 0.05$ *vs* Negative control. D. Western blot analyses of HER2, OPN, and EMT markers in GC cell line MKN45 and N87 after HER2-siRNA transfection. The protein level changes of these genes were consistent with the mRNA level changes.

as well as the down-regulated migratory and invasive potential. Knocking down HER2 led to similar changes in tumor invasion/migration and EMT markers. Meanwhile, the expression of OPN was down regulated after HER2 knockdown. These *in vitro* findings as well as results from the GC specimens indicated that OPN induced the acquisition of EMT in GCs, and it may be regulated by HER2 as a downstream molecule in the HER2 induced EMT process.

OPN plays important roles in various aspects to influence the biological behaviors of malignancies including the pathogenic development, progression and metastasis, *etc.* Kiss T et al. discovered that silencing OPN expression by siRNA decreased cell proliferation and invasion in melanoma [32]. Cao, D et al. indicated that OPN mediates multifaceted roles in the interaction between cancer cells and the tumor microenvironment, and OPN signaling results in various functions, including prevention of apoptosis, modulation of angiogenesis, malfunction of tumor-associated macrophages, activation of phosphoinositide 3-kinase-Akt (PI3K/AKT) pathways and NF-κB pathways, which lead to tumor formation and progression, particularly in gastric and liver cancers [17]. Lee J et al. found that OPN-CD44 interaction promotes extracellular matrix (ECM)-derived survival signal through integrin activation [13]. Down-regulation of OPN suppressed the growth, migration and invasion of GC cell line BGC-823 through the reduction of MMP-2 and uPA expression, inhibition of NF-κB DNA binding activities, and down-regulation of Akt phosphorylation [33]. OPN has been shown to promote invasion previously, but its role in EMT has not been elucidated in GCs. Dong Q *etc.* found that OPN can promote EMT in liver cancer by increasing the stability of vimentin [34]. However, in the current study, IHC analysis showed that vimentin was not expressed in GCs, indicating that OPN does not regulate EMT through vimentin in GCs. The findings in this study that OPN promotes the acquisition of EMT can provide a new aspect to elucidate the role and mechanisms of this marker in GCs.

The upstream regulation of OPN has not been clearly understood. Several studies showed that OPN was under the regulation of Wnt/β-catenin signal pathway [35–37]. Other factors including late SV40 factor (LSF) and NO has also been shown to participate in the regulation in hepatocellular carcinoma cell lines [38,39]. Nevertheless, little was known about the regulation of OPN in GCs. Our *in vitro* studies in GC cell lines, together with the histological findings in the GC specimen, proved the participation of OPN in HER2 mediated EMT process. To our knowledge, this study for the first time shows that HER2 participates in the upstream regulation of OPN. Since OPN has been proposed as a possible target for tumor treatments [15,33], the association between OPN and HER2 may suggested it would be a possible target option for

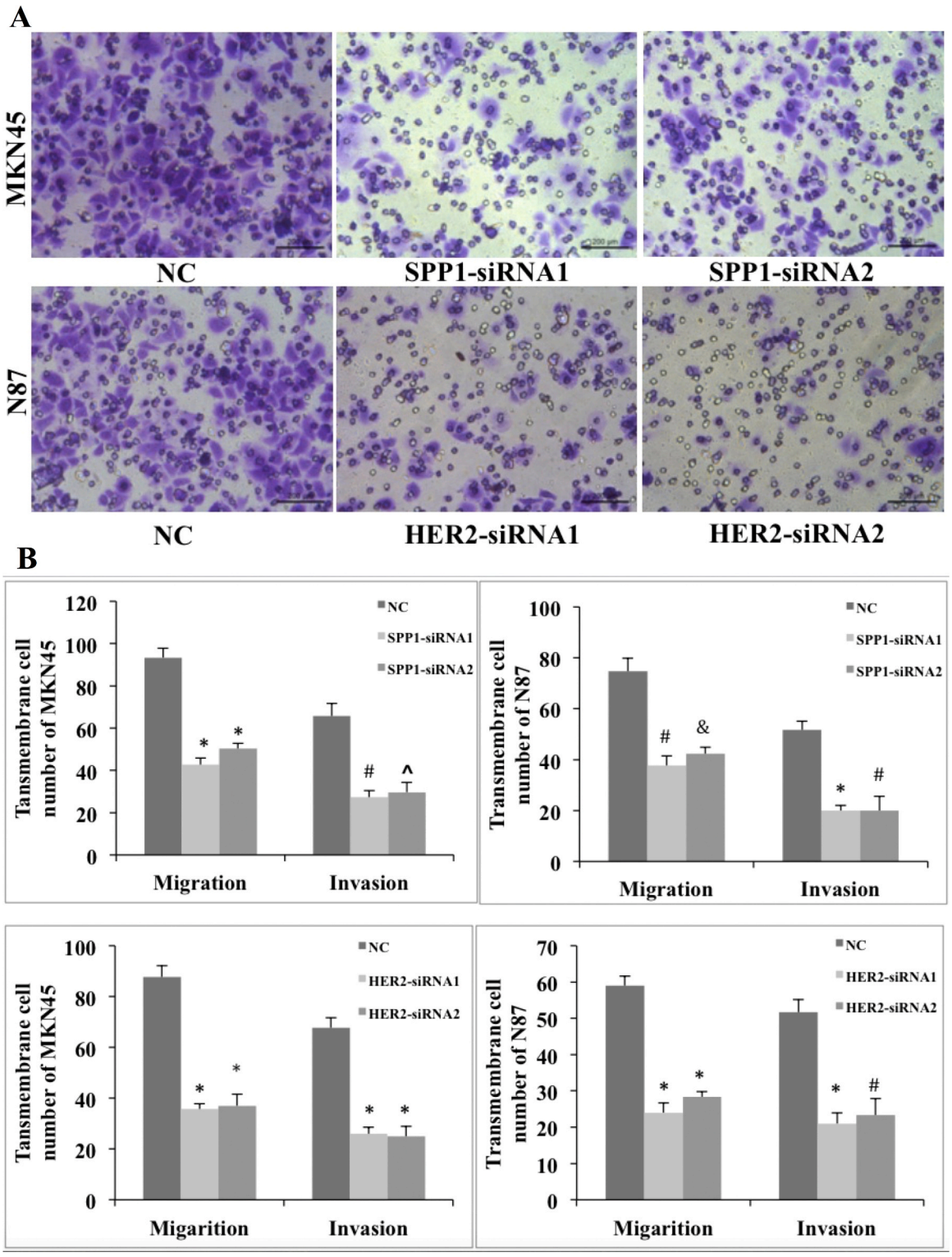

Fig. 5. Effects of SPP1 and HER2 knockdown on tumor migration and invasion in MKN45 and N87 cells. A. Representative images of transmembrane cells after SPP1 and HER2 siRNA transfection. The cells were stained with Giemsa. Magnification× 100. B. Comparison of migration and invasion after SPP1 and HER2 siRNA transfection. Inhibition of SPP1 and HER2 suppressed the migratory and invasive abilities in both cell lines. $^{*}P < 0.001$, $\#P = 0.001$, $\hat{}P = 0.002$, $^{\&}P = 0.003$ *vs* Negative control.

the treatment of HER2 positive GCs.

In conclusion, we found that OPN promotes the acquisition of EMT phenotype and the progressive behaviors, and this process is under the regulation of HER2 in GCs. These findings provide new insights on better understanding the roles, mechanisms and regulation of OPN and HER2 in tumor genesis, progression and metastasis in GCs. The underlying mechanism will be further explored in future studies.

CRediT authorship contribution statement

Liu Y mainly participated in most experiment operation and writing the initial manuscript. Chen L participated in the Nanostring analysis and the preliminary data processing. Jiang D participated in tissue microarray construction and IHC staining. Luan L helped to do the cell culture and PCR. Huang J helped to do the western blot and analyze the data. Hou Y was involved in the design, supervision of the study and modification of the manuscript. Xu C designed the study, supervised the study, analyzed the data and revised the manuscript. All authors read and approved the final manuscript.

Acknowledgment

The study was supported by the Shanghai Municipal Key Clinical Specialty, China (shslczdzk 01302); Shanghai Science and Technology Development Foundation, China (No. 19MC1911000); and the Foundation for Excellent Young Doctors of Zhongshan Hospital, China (2019ZSYXGG19).

Conflict of interest statement

The authors declared that they have no conflict of interest to this work.

Appendix A. Supporting information

Supplementary data associated with this article can be found in the online version at doi:10.1016/j.prp.2021.153643.

References

[1] L.A. Torre, F. Bray, R.L. Siegel, Global cancer statistics, 2012, CA Cancer J. Clin. 65 (2015) 87–108, https://doi.org/10.3322/caac.21262.
[2] P. Rawla, A. Barsouk, Epidemiology of gastric cancer: global trends, risk factors and prevention, Prz. Gastroenterol. 14 (2019) 26–38, https://doi.org/10.5114/pg.2018.80001.
[3] W. Chen, R. Zheng, P.D. Baade, Cancer statistics in China, 2015, CA Cancer J. Clin. 66 (2016) 115–132, https://doi.org/10.3322/caac.21338.
[4] Y.J. Bang, E. Van Cutsem, A. Feyereislova, Trastuzumab in combination with chemotherapy versus chemotherapy alone for treatment of HER2-positive advanced gastric or gastro-oesophageal junction cancer (ToGA): a phase 3, open-label, randomised controlled trial, Lancet 376 (2010) 687–697, https://doi.org/10.1016/S0140-6736(10)61121-X.
[5] J. Ruschoff, W. Hanna, M. Bilous, HER2 testing in gastric cancer: a practical approach, Mod. Pathol. 25 (2012) 637–650, https://doi.org/10.1038/modpathol.2011.198.
[6] J. Yang, H. Luo, Y. Li, Intratumoral heterogeneity determines discordant results of diagnostic tests for human epidermal growth factor receptor (HER) 2 in gastric cancer specimens, Cell Biochem. Biophys. 62 (2012) 221–228, https://doi.org/10.1007/s12013-011-9286-1.
[7] E.Y. Cho, K. Park, I. Do, Heterogeneity of ERBB2 in gastric carcinomas: a study of tissue microarray and matched primary and metastatic carcinomas, Mod. Pathol. 26 (2013) 677–684, https://doi.org/10.1038/modpathol.2012.205.
[8] F. Grillo, M. Fassan, F. Sarocchi, HER2 heterogeneity in gastric/gastroesophageal cancers: From benchside to practice, World J. Gastroenterol. 22 (2016) 5879–5887, https://doi.org/10.3748/wjg.v22.i26.5879.
[9] Y.J. Liu, D.Q. Zhang, X.M. Sui, Overexpression of human osteopontin increases cell proliferation and migration in human embryo kidney-293 cells, Cell Mol. Biol. Lett. 14 (2009) 670–678, https://doi.org/10.2478/s11658-009-0027-z.
[10] H. Rangaswami, A. Bulbule, G.C. Kundu, Osteopontin: role in cell signaling and cancer progression, Trends Cell Biol. 16 (2006) 79–87, https://doi.org/10.1016/j.tcb.2005.12.005.
[11] J.W. Park, S.H. Lee, M. Go du, Osteopontin depletion decreases inflammation and gastric epithelial proliferation during Helicobacter pylori infection in mice, Lab. Invest. 95 (2015) 660–671, https://doi.org/10.1038/labinvest.2015.47.
[12] Y.L. Chai, J.R. Chong, A.R. Raquib, Plasma osteopontin as a biomarker of Alzheimer's disease and vascular cognitive impairment, Sci. Rep. 11 (2021) 4010, https://doi.org/10.1038/s41598-021-83601-6.
[13] J.L. Lee, M.J. Wang, P.R. Sudhir, Osteopontin promotes integrin activation through outside-in and inside-out mechanisms: OPN-CD44V interaction enhances survival in gastrointestinal cancer cells, Cancer Res. 67 (2007) 2089–2097, https://doi.org/10.1158/0008-5472.can-06-3625.
[14] L.A. Shevde, S. Das, D.W. Clark, Osteopontin: an effector and an effect of tumor metastasis, Curr. Mol. Med. 10 (2010) 71–81, https://doi.org/10.2174/156652410791065381.
[15] H.R. Moorman, D. Poschel, J.D. Klement, Osteopontin: a key regulator of tumor progression and immunomodulation, Cancers 12 (2020), https://doi.org/10.3390/cancers12113379.
[16] Z.M. Wang, Y.H. Cui, W. Li, Lentiviral-mediated siRNA targeted against osteopontin suppresses the growth and metastasis of gastric cancer cells, Oncol. Rep. 25 (2011) 997–1003, https://doi.org/10.3892/or.2011.1168.
[17] D.X. Cao, Z.J. Li, X.O. Jiang, Osteopontin as potential biomarker and therapeutic target in gastric and liver cancers, World J. Gastroenterol. 18 (2012) 3923–3930, https://doi.org/10.3748/wjg.v18.i30.3923.
[18] M. Katoh, Epithelial-mesenchymal transition in gastric cancer (Review), Int. J. Oncol. 27 (2005) 1677–1683.
[19] Y. Shi, D. He, Y. Hou, An alternative high output tissue microarray technique, Diagn. Pathol. 8 (2013) 9, https://doi.org/10.1186/1746-1596-8-9.
[20] M. Hofmann, O. Stoss, D. Shi, Assessment of a HER2 scoring system for gastric cancer: results from a validation study, Histopathology 52 (2008) 797–805, https://doi.org/10.1111/j.1365-2559.2008.03028.x.
[21] J. Ruschoff, M. Dietel, G. Baretton, HER2 diagnostics in gastric cancer-guideline validation and development of standardized immunohistochemical testing, Virchows Arch. 457 (2010) 299–307, https://doi.org/10.1007/s00428-010-0952-2.
[22] K.M. Kim, M. Bilous, K.M. Chu, Human epidermal growth factor receptor 2 testing in gastric cancer: recommendations of an Asia-Pacific task force, Asia Pac. J. Clin. Oncol. 10 (2014) 297–307, https://doi.org/10.1111/ajco.12263.
[23] R.A. Soslow, A.J. Dannenberg, D. Rush, COX-2 is expressed in human pulmonary, colonic, and mammary tumors, Cancer 89 (2000) 2637–2645.
[24] T.D. Schmittgen, B.A. Zakrajsek, A.G. Mills, Quantitative reverse transcription-polymerase chain reaction to study mRNA decay: comparison of endpoint and real-time methods, Anal. Biochem. 285 (2000) 194–204, https://doi.org/10.1006/abio.2000.4753.
[25] Y.Q. Shan, R.C. Ying, C.H. Zhou, MMP-9 is increased in the pathogenesis of gastric cancer by the mediation of HER2, Cancer Gene Ther. 22 (2015) 101–107, https://doi.org/10.1038/cgt.2014.61.
[26] T. Ue, H. Yokozaki, Y. Kitadai, Co-expression of osteopontin and CD44v9 in gastric cancer, Int. J. Cancer 79 (1998) 127–132, https://doi.org/10.1002/(sici)1097-0215(19980417)79:2<127::aid-ijc5>3.0.co;2-v.
[27] M. Higashiyama, T. Ito, E. Tanaka, Prognostic significance of osteopontin expression in human gastric carcinoma, Ann. Surg. Oncol. 14 (2007) 3419–3427, https://doi.org/10.1245/s10434-007-9564-8.
[28] N. Dai, Q. Bao, A. Lu, Protein expression of osteopontin in tumor tissues is an independent prognostic indicator in gastric cancer, Oncology 72 (2007) 89–96, https://doi.org/10.1159/000111108.
[29] R.X. Chen, Y.H. Xia, J.F. Cui, Osteopontin, a single marker for predicting the prognosis of patients with tumor-node-metastasis stage I hepatocellular carcinoma after surgical resection, J. Gastroenterol. Hepatol. 25 (2010) 1435–1442, https://doi.org/10.1111/j.1440-1746.2010.06277.x.
[30] A.N. Bartley, M.K. Washington, C.B. Ventura, HER2 testing and clinical decision making in gastroesophageal adenocarcinoma: guideline from the College of American Pathologists, American Society for Clinical Pathology, and American Society of Clinical Oncology, Arch. Pathol. Lab Med. 140 (2016) 1345–1363, https://doi.org/10.5858/arpa.2016-0331-CP.
[31] L. Huang, R.L. Wu, A.M. Xu, Epithelial-mesenchymal transition in gastric cancer, Am. J. Transl. Res. 7 (2015) 2141–2158.
[32] T. Kiss, K. Jámbor, V. Koroknai, Silencing osteopontin expression inhibits proliferation, invasion and induce altered protein expression in melanoma cells, Pathol. Oncol. Res. 27 (2021), 581395, https://doi.org/10.3389/pore.2021.581395.
[33] M. Gong, Z. Lu, G. Fang, A small interfering RNA targeting osteopontin as gastric cancer therapeutics, Cancer Lett. 272 (2008) 148–159, https://doi.org/10.1016/j.canlet.2008.07.004.
[34] Q. Dong, X. Zhu, C. Dai, Osteopontin promotes epithelial-mesenchymal transition of hepatocellular carcinoma through regulating vimentin, Oncotarget 7 (2016) 12997–13012, https://doi.org/10.18632/oncotarget.7016.
[35] H. Tang, J. Wang, F. Bai, Positive correlation of osteopontin, cyclooxygenase-2 and vascular endothelial growth factor in gastric cancer, Cancer Invest. 26 (2008) 60–67, https://doi.org/10.1080/07357900701519279.
[36] R. Zagani, N. Hamzaoui, W. Cacheux, Cyclooxygenase-2 inhibitors down-regulate osteopontin and Nr4A2-new therapeutic targets for colorectal cancers, Gastroenterology 137 (2009) 1358–1366, https://doi.org/10.1053/j.gastro.2009.06.039 (e1351-1353).
[37] A. Mitra, M.E. Menezes, L.K. Pannell, DNAJB6 chaperones PP2A mediated dephosphorylation of GSK3β to downregulate β-catenin transcription target, osteopontin, Oncogene 31 (2012) 4472–4483, https://doi.org/10.1038/onc.2011.623.
[38] H. Guo, C.E. Marroquin, P.Y. Wai, Nitric oxide-dependent osteopontin expression induces metastatic behavior in HepG2 cells, Dig. Dis. Sci. 50 (2005) 1288–1298, https://doi.org/10.1007/s10620-005-2775-6.
[39] B.K. Yoo, L. Emdad, R. Gredler, Transcription factor Late SV40 Factor (LSF) functions as an oncogene in hepatocellular carcinoma, Proc. Natl. Acad. Sci. USA 107 (2010) 8357–8362, https://doi.org/10.1073/pnas.1000374107.